

Civil Engineering Journal

(E-ISSN: 2476-3055; ISSN: 2676-6957)

Vol. 11, No. 10, October, 2025



Development of Sustainable Self-Compacting Concrete Using Slag Sand and Expanded Clay Aggregates

Usha Rani Bala 1*, R. Bhavani 10, J. Guru Jawahar 20

¹ Department of Civil Engineering, Jawaharlal Nehru Technological University, Andhra Pradesh, Ananthapur, 515002, India.

² Department of Civil Engineering, Annamacharya Institute of Technology and Sciences, Tirupati, India.

Received 12 June 2025; Revised 12 September 2025; Accepted 19 September 2025; Published 01 October 2025

Abstract

The objective of this study is to develop a sustainable self-compacting concrete (SCC) by partially replacing natural aggregates with slag sand (SS) and lightweight expanded clay aggregate (ECA) in combination with a ternary binder system, thereby enhancing both performance and environmental sustainability. The methodology involved preparing thirty SCC mixes of M30 grade using 65% Ordinary Portland Cement, 25% fly ash, and 10% silica fume as binder, with slag sand replacing river sand at 20–100% and ECA replacing coarse aggregate at 20–100%. Fresh properties were evaluated through slump flow, T50, V-funnel, L-box, and U-box tests following EFNARC guidelines, while mechanical strength (compressive, split tensile, and flexural) was measured at 7, 28, and 90 days. Durability was assessed through sulphuric acid and magnesium sulphate exposure, and microstructural behavior was studied using FTIR and TGA. Results revealed that mixes with higher ECA content enhanced flowability, with A2B10 achieving superior workability (slump flow 694 mm, T50 2.9 s), while A2B6 (20% SS + 20% ECA) achieved optimum strength (45.21 MPa compressive) and durability retention under aggressive exposures. The novelty of this work lies in demonstrating the synergistic role of slag sand and ECA in producing SCC with enhanced performance, reduced natural aggregate usage, and improved sustainability compared to conventional SCC.

Keywords: Self-Compacting Concrete; Fresh Properties of Concrete; Mechanical Properties of Concrete; Durability and Micro Structural Properties of Concrete; Ternary Binder.

1. Introduction

Self-compacting concrete (SCC) has emerged as a revolutionary construction material due to its ability to flow under its own weight, fill congested reinforcement, and achieve complete compaction without vibration. This property not only reduces labor and noise pollution but also improves construction quality and durability [1, 2]. In addition, SCC offers opportunities for sustainability by incorporating supplementary cementitious materials (SCMs) and industrial byproducts, thereby minimizing reliance on ordinary Portland cement (OPC) and natural aggregates [3–5]. Lightweight expanded clay aggregate (ECA) has been recognized as a promising coarse aggregate replacement because of its spherical shape, low density, and porous texture. These properties reduce structural dead load, enhance thermal insulation, and promote better flow in congested formworks [6–8]. Similarly, slag sand, a by-product of steel manufacturing, has been successfully used as a fine aggregate substitute. Its angular particles and latent pozzolanic reactivity improve cohesiveness, filling ability, and long-term strength [9–11].

The combined use of fly ash, silica fume, slag sand, and lightweight aggregates in SCC therefore aligns with the dual goals of enhancing performance and promoting sustainability [12–15]. Recent studies have further reinforced the

^{*} Corresponding author: ushasscjntua@gmail.com



http://dx.doi.org/10.28991/CEJ-2025-011-10-015

© 2025 by the authors. Licensee C.E.J, Tehran, Iran. This article is an open access article distributed under the terms and conditions of the Creative Commons Attribution (CC-BY) license (http://creativecommons.org/licenses/by/4.0/).

role of sustainable materials in SCC. The use of ground ferronickel slag (GFNS) as a fine aggregate has been shown to enhance rheological and microstructural properties when incorporated up to 20% replacement levels [16]. Recycled concrete aggregates (RCA) have also been demonstrated to effectively substitute both fine and coarse aggregates while maintaining satisfactory performance when proper water adjustments are applied [17]. Ternary blended SCC incorporating steel slag and calcined kaolinitic clay exhibited improved strength and sulphate resistance, highlighting the potential of multi-component binder systems [18]. Long-term investigations of sustainable SCC have further emphasized the importance of extended durability assessments to fully validate performance [19, 20]. In lightweight concrete development, artificial aggregates manufactured from clay, rice husk ash, and glass powder have been successfully employed to produce structural lightweight SCC [21, 22], while bibliometric reviews have mapped research progress and trends in the use of recycled aggregates [23, 24]. In addition, replacing fine aggregates with an equal blend of sea sand and manufactured sand was found to significantly enhance compressive strength and chloride resistance at 90 days [25, 26]. Collectively, these studies underline the global shift toward sustainable alternatives in SCC, demonstrating the feasibility of industrial by-products and engineered aggregates in improving both performance and environmental outcomes.

The performance of self-compacting concrete (SCC) incorporating slag sand, expanded clay aggregate (ECA), and a ternary binder system can be explained through fundamental mechanisms related to particle packing, hydration, and durability [25, 26]. Slag sand, with its finer particle size and angularity compared to natural sand, improves the packing density of the mix and reduces voids, thereby enhancing rheology and cohesiveness [27, 28]. This refined particle arrangement minimizes segregation and facilitates the self-compacting behavior required for SCC [29]. The ternary binder system, consisting of OPC, fly ash, and silica fume, further contributes to performance by combining the rapid pozzolanic activity of silica fume, which refines pore structure and strengthens the matrix at early ages, with the slower pozzolanic activity of fly ash, which sustains hydration and strength development at later ages [30, 31]. Together, these materials increase the formation of calcium silicate hydrate (C-S-H) and reduce calcium hydroxide, leading to a denser and more durable microstructure. The addition of ECA provides another advantage, as its porous structure absorbs water during mixing and releases it gradually during hydration, offering an internal curing effect that mitigates autogenous shrinkage and supports long-term hydration [32]. The spherical shape of ECA particles also contributes to improved flow and reduced risk of blockage in congested reinforcement zones [6]. In terms of durability, the combined effects of refined pore structure from slag sand and silica fume, pozzolanic reactions from fly ash, and internal curing from ECA lead to reduced permeability, minimized microcracking, and improved resistance against chemical attack [33-36]. From a sustainability perspective, the replacement of river sand with slag sand and natural coarse aggregates with ECA reduces the depletion of natural resources, diverts industrial by-products from landfills, and lowers the overall environmental footprint [37]. Thus, the theoretical framework demonstrates that the hybrid uses of slag sand, ECA, and a ternary binder system can synergistically improve fresh properties, strength, durability, and sustainability of SCC compared to conventional mixtures.

Despite these advances, limited research has comprehensively investigated SCC mixes that simultaneously employ slag sand as fine aggregate, ECA as coarse aggregate, and a ternary binder system (OPC–fly ash–silica fume). Moreover, very few studies assess performance under aggressive chemical exposures or integrate microstructural analysis to explain observed behaviors. This creates a critical gap in understanding the synergistic effects of combining slag sand and ECA in SCC. The present study aims to address these gaps by (i) investigating the fresh properties of SCC mixes incorporating slag sand and ECA in varying proportions, in accordance with EFNARC guidelines; (ii) evaluating mechanical properties such as compressive, split tensile, and flexural strength; (iii) assessing durability performance under acid and sulphate exposures; and (iv) analyzing microstructural features through Fourier Transform Infrared Spectroscopy (FTIR) and Thermogravimetric Analysis (TGA).

The remainder of this article is structured as follows. Section 2 describes the materials, mix proportions, and experimental methodology. Section 3 presents the results of fresh, mechanical, durability, and microstructural investigations, followed by detailed discussions. Section 4 summarizes the conclusions and outlines directions for future research. The references cited throughout the manuscript are compiled at the end.

2. Materials and Methodology

2.1. Materials Used

2.1.1. Ternary Cementitious Binders

The primary binder in this study was Ordinary Portland Cement (OPC) of 53-grade, which was obtained from UltraTech Company and had a specific gravity of 3.12, a fineness of 4.16%, a standard consistency of 29%, and initial and final setting times of 110 mins and 241 mins, respectively. Class F fly ash with specific gravity 2.2, sourced from the Rayalaseema Thermal Power Plant near Muddhanuru, Andhra Pradesh, and silica fume supplied by Astraa Chemicals in Hyderabad, Telangana, were both used to partially replace the cement.

2.1.2. Fine Aggregates

Natural river sand, sourced locally from quarries in the Ananthapuram district of Andhra Pradesh, served as the fine aggregate and exhibited a specific gravity of 2.65, water absorption of 0.8%, and a fineness modulus of 2.68; its particle size distribution conforms to Zone II. Slag sand, a steel-manufacturing by-product supplied by the JSW Steel Plant in Bellary, Karnataka, was used as an alternative fine aggregate. It has a specific gravity of 2.55, absorbs 0.9% water, and possesses a fineness modulus of 2.6, with its grading also meeting Zone II requirements.

The gradation of river sand and slag sand was determined per IS 383:2016. Figure 1 presents the cumulative passing curves alongside the IS 383:2016 Zone II envelope; both aggregates satisfy Zone II requirements, with slag sand showing a slightly finer tail that supports improved packing.

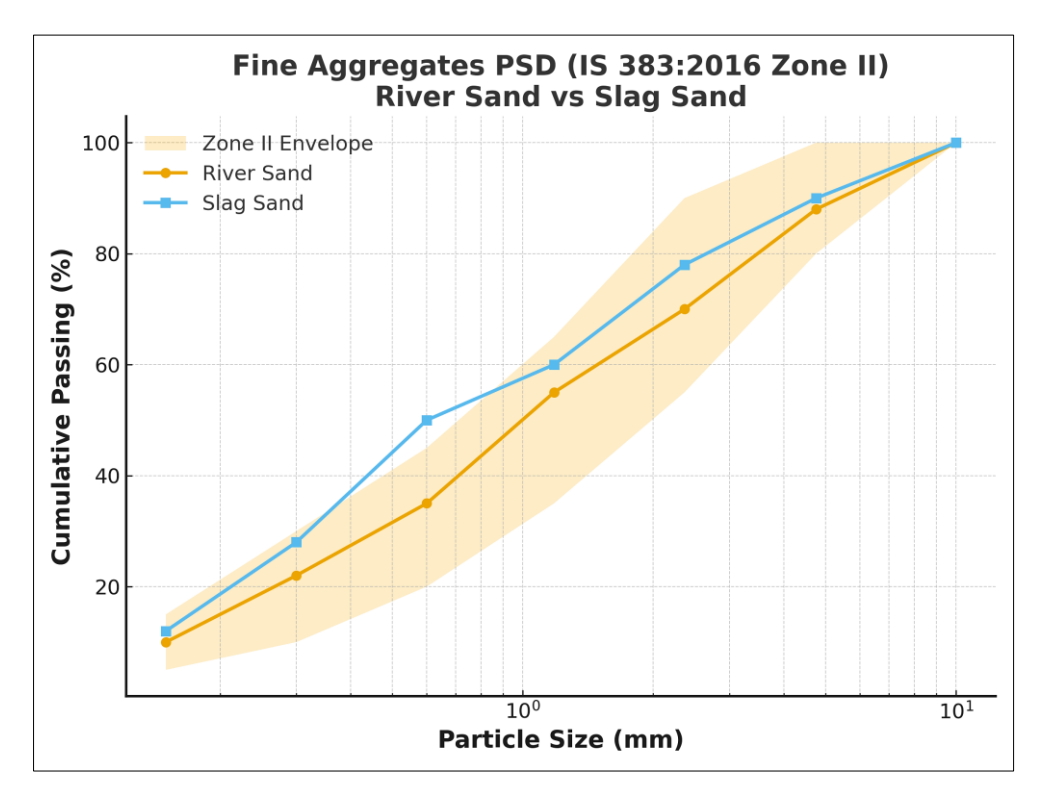


Figure 1. Particle size distribution (PSD) of fine aggregates (river sand and slag sand) with IS 383:2016 Zone II grading envelope

2.1.3. Coarse Aggregate

Crushed granite stones of size 10 mm and 20 mm were used as coarse aggregate, with a specific gravity of 2.72 and water absorption of 0.4%. Expanded Clay Aggregates (ECA), sourced from Hyderabad, were utilized as a substitute for conventional coarse aggregates, with a specific gravity of 2.72 and water absorption of 0.4%.

The particle size distribution (PSD) of coarse aggregates was determined per IS 383:2016. As shown in Table 1 and Figure 2, the 10 mm nominal granite demonstrates 100% passing through the 20 mm sieve, 81.5% at 12.5 mm, and 51.8% at 10 mm. In comparison, the 20 mm nominal granite shows coarser gradation (27.1% passing at 12.5 mm, 4.6% at 10 mm). The expanded clay aggregate (ECA) exhibits a more uniform and finer distribution, reflecting its porous and lightweight nature. This distinct gradation influences the packing density and contributes to internal curing in SCC mixes.

Table 1. Particle size distribution (PSD) of coarse aggregates (granite 10 mm, granite 20 mm, and expanded clay aggregate – ECA)

S. No.	Mix	Cement (%)	Flyash (%)	Silica fume (%)
1	80 mm	100	100	100
2	40 mm	100	100	100
3	20 mm	100	100	100
4	12.5 mm	81.5	27.117	64
5	10 mm	51.82	4.634	51
6	4.75 mm	19.94	0.01	30
7	PAN	0.04	-	7

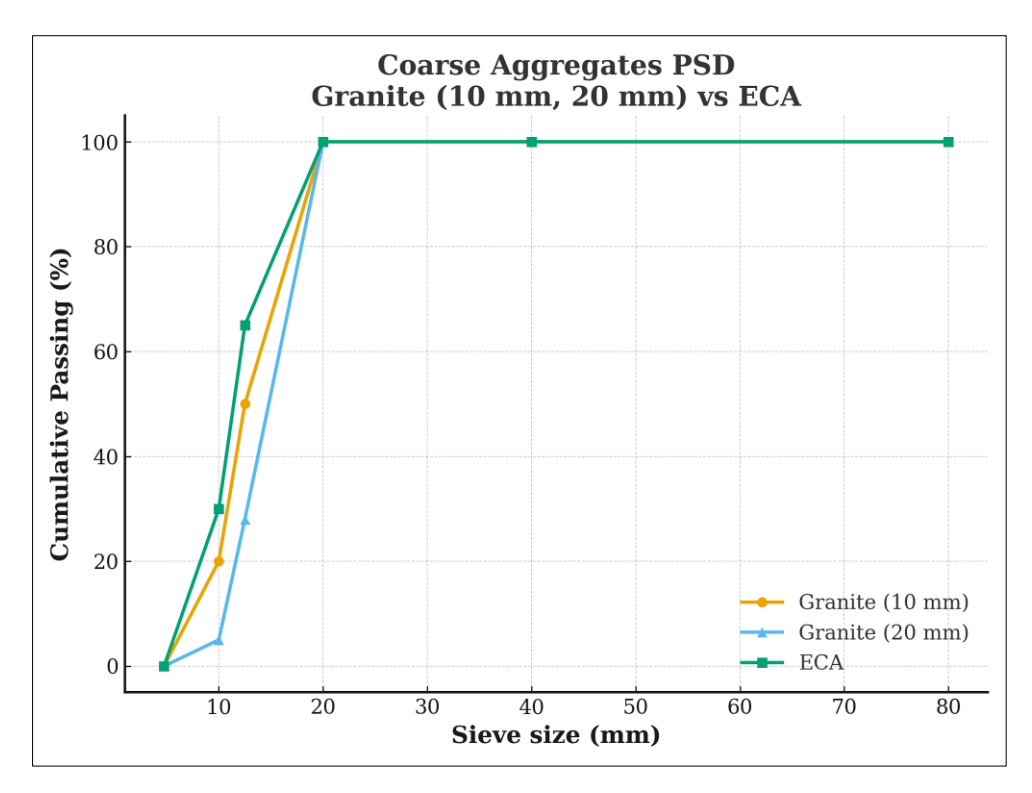


Figure 2. Particle size distribution (PSD) of coarse aggregates: granite (10 mm and 20 mm nominal) and expanded clay aggregate (ECA)

The combined effect of these materials results in improved particle packing density, reduced segregation, and enhanced rheology, all of which are essential for self-compacting concrete. The gradation also influences the interfacial transition zone (ITZ) between paste and aggregates, directly impacting strength and durability. The use of slag sand as fine aggregate replacement enhances cohesion and reduces bleeding, while ECA provides reduced density and sustained hydration through its water absorption and release mechanism.

2.1.4. Water

From mixing to curing, clean, potable water was continuously used in the concrete production process.

2.1.5. Chemical Admixtures

Ether (PCE)-based chemical admixture was used as a superplasticizer and obtained from BASF Construction Chemicals, Hyderabad, Telangana, India.

2.2. Mix Proportions

A total of 30 combinations were formulated for M30-grade self-compacting concrete (SCC) Each mix incorporated a ternary binder system consisting of 294 kg/m³ ordinary Portland cement (OPC), 113 kg/m³ fly ash, and 45 kg/m³ silica fume, maintained constantly across all mixes, FA (887 kg/m³), CA (1010 kg/m³), water (158 lt/m³), and chemical admixture (2%). Various percentages of slag sand and lightweight expanded clay aggregate were used, combined with a ternary binder and its mix designations were shown in Table 2. The Mixes A2 to A6 were considered as baseline mixes to assess the individual effect of slag sand. Intermediate ranges (10–15%) were initially considered during trial batches, but 20% levels were finalized due to superior workability and mechanical performance. Lower substitutions did not produce significant benefits compared to control mixes.

2.3. Experimental Program

The experimental study involved the assessment of the fresh and hardened properties, as well as the durability characteristics, of SCC. The details of the tests performed were discussed in the following sections and the schematic representation of the developments of sustainable SCC was illustrated in Figure 3.

Table 2. Mix proportions and designations

S.No.	Mix	Cement (%)	Flyash (%)	Silica fume (%)	FA (%)	SS (%)	CA (%)	ECA (%)	Water (%)	SP (%)
1	A2	65%	25%	10%	80%	20%	100%	0%	0.42	2%
2	A3	65%	25%	10%	60%	40%	100%	0%	0.42	2%
3	A4	65%	25%	10%	40%	60%	100%	0%	0.42	2%
4	A5	65%	25%	10%	20%	80%	100%	0%	0.42	2%
5	A6	65%	25%	10%	0%	100%	100%	0%	0.42	2%
6	A2B6	65%	25%	10%	80%	20%	80%	20%	0.42	2%
7	A2B7	65%	25%	10%	80%	20%	60%	40%	0.42	2%
8	A2B8	65%	25%	10%	80%	20%	40%	60%	0.42	2%
9	A2B9	65%	25%	10%	80%	20%	20%	80%	0.42	2%
10	A2B10	65%	25%	10%	80%	20%	0%	100%	0.42	2%
11	A3B6	65%	25%	10%	60%	40%	80%	20%	0.42	2%
12	A3B7	65%	25%	10%	60%	40%	60%	40%	0.42	2%
13	A3B8	65%	25%	10%	60%	40%	40%	60%	0.42	2%
14	A3B9	65%	25%	10%	60%	40%	20%	80%	0.42	2%
15	A3B10	65%	25%	10%	60%	40%	0%	100%	0.42	2%
16	A4B6	65%	25%	10%	40%	60%	80%	20%	0.42	2%
17	A4B7	65%	25%	10%	40%	60%	60%	40%	0.42	2%
18	A4B8	65%	25%	10%	40%	60%	40%	60%	0.42	2%
19	A4B9	65%	25%	10%	40%	60%	20%	80%	0.42	2%
20	A4B10	65%	25%	10%	40%	60%	0%	100%	0.42	2%
21	A5B6	65%	25%	10%	20%	80%	80%	20%	0.42	2%
22	A5B7	65%	25%	10%	20%	80%	60%	40%	0.42	2%
23	A5B8	65%	25%	10%	20%	80%	40%	60%	0.42	2%
24	A5B9	65%	25%	10%	20%	80%	20%	80%	0.42	2%
25	A5B10	65%	25%	10%	20%	80%	0%	100%	0.42	2%
26	A6B6	65%	25%	10%	0%	100%	80%	20%	0.42	2%
27	A6B7	65%	25%	10%	0%	100%	60%	40%	0.42	2%
28	A6B8	65%	25%	10%	0%	100%	40%	60%	0.42	2%
29	A6B9	65%	25%	10%	0%	100%	20%	80%	0.42	2%
30	A6B10	65%	25%	10%	0%	100%	0%	100%	0.42	2%



Figure 3. Schematic representation of the development of sustainable $\ensuremath{\mathsf{SSC}}$

2.3.1. Fresh Properties

The fresh properties of the SCC mixes were assessed based on EFNARC recommendations through a series of tests, including Slump Flow, T50 Slump Flow, V-Funnel, L-Box, and U-Box [33].

- Slump Flow test: This test was conducted to evaluate the flowability and workability of the self-compacting concrete (SCC) mixes. Fresh SCC was poured into a standard slump cone, and upon lifting the cone, the horizontal spread of the concrete was measured to determine its ability to flow under its own weight without segregation.
- **T50 slump flow test**: It was performed to assess the viscosity characteristics of self-compacting concrete (SCC), the amount of time it took for the concrete to spread across a 50 cm diameter was recorded. As per EFNARC the acceptable range is 2 to 5 seconds. [33, 34].
- V funnel test It is performed to evaluate the viscosity and flowability of the concrete by measuring the time it took for the mix to pass through a V-shaped funnel under its own weight. A flow time of 6 to 12 seconds is usually acceptable [33].
- **L-box test:** The L-box apparatus measures how well SCC can flow through a reinforcing-bar matrix by filling its vertical and horizontal sections and comparing the concrete heights. The resulting blocking ratio (H₂/H₁) quantifies this ability, with ratios of 0.8 to 1.0 indicating acceptable performance [33, 34].
- **U Box test:** The U-box test assesses the passing ability of SCC by measuring the height difference between two chambers after the flow through reinforcement. The permissible height difference is generally 0–30 mm [33, 34].

2.3.2. Mechanical Properties

The following tests were performed on the concrete samples to assess the mechanical properties of SCC.

• Compressive strength test: Total of 270 cube samples of size 150 mm × 150 mm × 150 mm were made (shown in Figure 4) and tested in compliance with IS 516:2013 [35]. Three specimens were prepared for each mixture and curing duration of 7, 28, and 90 days in order to ensure result accuracy. Subsequent to the designated curing durations, the cubes were surface-dried and evaluated with a calibrated compression testing apparatus to measure the compressive strength. The mean of three measurements was considered the representative value for each age [36].



Figure 4. Casted samples

- Split tensile strength test: Total of 270-cylinder samples of size 150 mm × 300 mm were made (shown in Figure 2) and tested in compliance with IS 516:2013 [36]. To ensure the accuracy of results, three specimens were made for each mix with curing ages of 7, 28, and 90 days. After curing, the specimens were surface-dried and subjected to diametral compression using a calibrated testing machine. The average tensile strength, calculated from three specimens, was used as the representative value for each curing age [38].
- Flexural strength test: 270 Beam specimens of size 100 mm × 100 mm × 500 mm were made and tested for flexural strength in accordance with IS code IS 516:2013 [18]. Three specimens were evaluated for each mix and age group of 7, 28, and 90 days, utilizing the two-point loading method. Following the curing process, the beams were dried and subjected to loading until failure occurred. The modulus of rupture was determined, and the mean of three results were recorded as the flexural strength at each age [23].

2.3.3. Durability Properties

To evaluate the durability of Self-Compacting Concrete (SCC) mixes under aggressive chemical environments, after 28 days of water curing, the specimens were tested for acid and sulphate attack. For the acid resistance test, concrete cubes were immersed in a 5% sulphuric acid (H₂SO₄) solution, while for the sulphate resistance test, similar specimens were immersed in a 5% magnesium sulphate (MgSo₄) solution. The specimens remained in these solutions for extended periods, and compressive strength tests were conducted at both 28 and 90 days of exposure. The percentage loss in strength was determined by comparing the results with those of control specimens cured in water. These procedures were conducted in accordance with the guidelines provided in IS 516:1959.

2.3.4. Microstructural Analysis

The following tests were performed on the concrete samples to assess the Microstructural Analysis of SCC.

• Fourier Transform Infrared Spectroscopy (FTIR)

Microstructural characterization was performed to understand the hydration phases and chemical bonds in the SCC mixes. Powdered samples from the control (A2), optimum mix (A2B6), and high-replacement mix (A2B10) were dried at 60° C to remove free water, sieved to pass through 90 µm, and analyzed using a Bruker Alpha II FTIR spectrometer. Scans were recorded between 4000 cm^{-1} and 400 cm^{-1} at a resolution of 4 cm⁻¹ with 32 scans per sample. This allowed the identification of peaks related to C–S–H gel, portlandite, and carbonate phases

• Thermogravimetric Analysis (TGA/DTG)

Thermal analysis was carried out using a Mettler Toledo TGA/DSC 1 analyzer. About 20 mg of each dried sample was heated from ambient temperature to 1000°C at a rate of 10°C/min in a nitrogen atmosphere. The mass losses were analyzed in three temperature ranges:

- 50–200°C: Evaporation of physically bound water and dehydration of C–S–H gel.
- 400–500°C: De-hydroxylation of Ca(OH)₂ (portlandite).
- 600-800 °C: Decarbonation of CaCO₃ .

3. Results and Discussion

The concrete specimens were tested according to standard procedures. The experimental data obtained from these tests were systematically analyzed, and the results were presented graphically. The results were carefully assessed to understand the impact of various material blends on the fresh and mechanical behavior of the mixes. The detailed analysis and discussions are provided in the following sections.

3.1. Fresh Properties

Slump flow test: The effect of 20%, 40%, 60%, 80%, and 100% slag sand, combined with increasing proportions of expanded clay aggregate (ECA), is analyzed below and depicted in Figure 5. The reference mixes A2 to A6 exhibit slump flow values ranging from 558 mm to 568 mm, all of which are below the EFNARC-recommended good workable range of 650 mm. This indicates that these mixes, despite varying the fine aggregate (FA) and silica sand (SS) content, do not meet the required flowability for SCC. The limited flow is attributed to the presence of conventional coarse aggregate (CA), which creates internal resistance, and the absence of more flow-enhancing materials. The addition of Expanded Clay Aggregate (ECA) in mixes A2B6 to A6B10, as a partial to full replacement of conventional coarse aggregate, shows a clear and consistent improvement in slump flow values across all series. As the ECA content increases from 20% to 100%, the flowability of the concrete significantly improves, with several mixes exceeding the EFNARC minimum requirement of 650 mm. Notable results include A2B10 (694 mm), A3B10 (692 mm), and A4B10 (676 mm), all of which demonstrate excellent filling ability suitable for self-compacting applications. Even the A6 series, which initially had the lowest slump flow (568 mm), reaches 652 mm at full ECA replacement (A6B10), just above the EFNARC threshold. This positive trend is attributed to the unique characteristics of ECA its lightweight, rounded shape, and porous texture which help reduce internal friction among particles, thus enhancing the mix's deformability and eliminating the need for external compaction [39, 40].

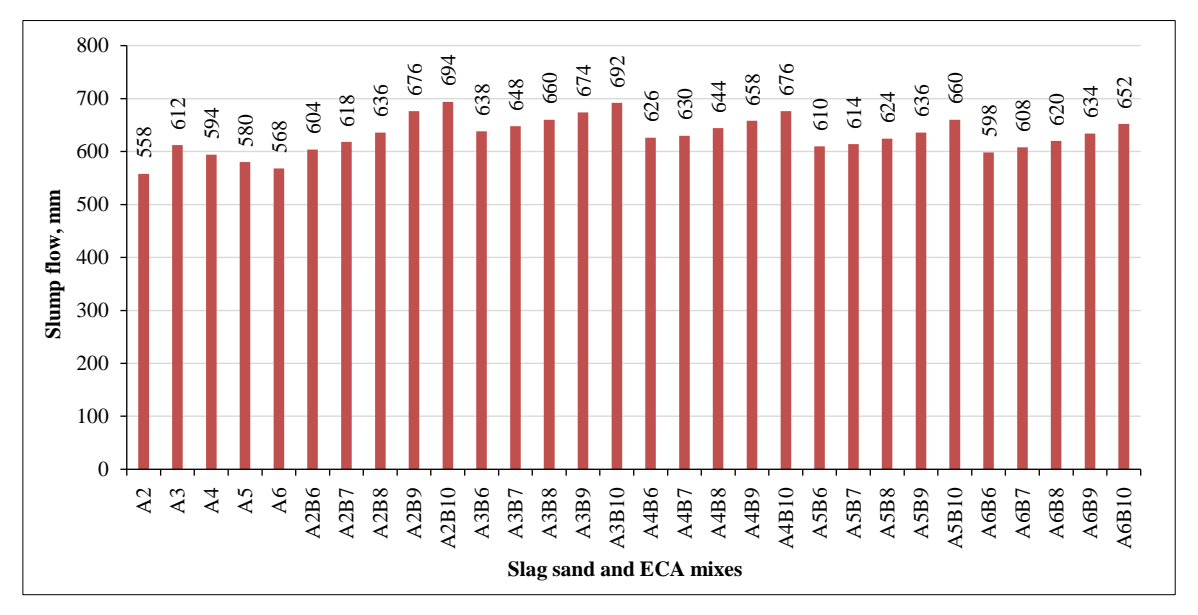


Figure 5. variation of Slump flow with slag sand and ECA mixes

T50 Slump flow test: The effect of 20%, 40%, 60%, 80%, and 100% slag sand, combined with increasing proportions of expanded clay aggregate (ECA), is analyzed below and depicted in Figure 6. The T50 slump flow results reveal a clear trend in how the inclusion of Expanded Clay Aggregate (ECA) influences the viscosity and filling ability of Self-Compacting Concrete (SCC). Reference mixes A2 to A6, which do not contain ECA, show higher T50 values ranging from 4.6 to 4.9 seconds, indicating slower flow and higher viscosity. As ECA replaces coarse aggregate in increasing proportions from 20% to 100% (A2B6 to A6B10), the T50 time decreases, reflecting improved flowability and reduced resistance to deformation. Notably, mix A2B10 achieves the lowest T50 value of 2.9 seconds, suggesting the most fluid and easily flowing mix, followed by A2B9 (3.01 s), A3B10 (3.24 s), and A3B9 (3.35 s), all of which fall well within the EFNARC-recommended range of 2 to 5 seconds. These mixes demonstrate optimal viscosity and self-compacting performance. However, in the A6 series, a slight increase in T50 values is observed at higher ECA levels, though still within acceptable limits (A6B10: 4.09 s). Based on the results, the optimum performance in terms of viscosity and flow is achieved at or near 20–100% ECA replacement, with A2B10 emerging as the most effective mix for maximizing flow while maintaining EFNARC compliance.

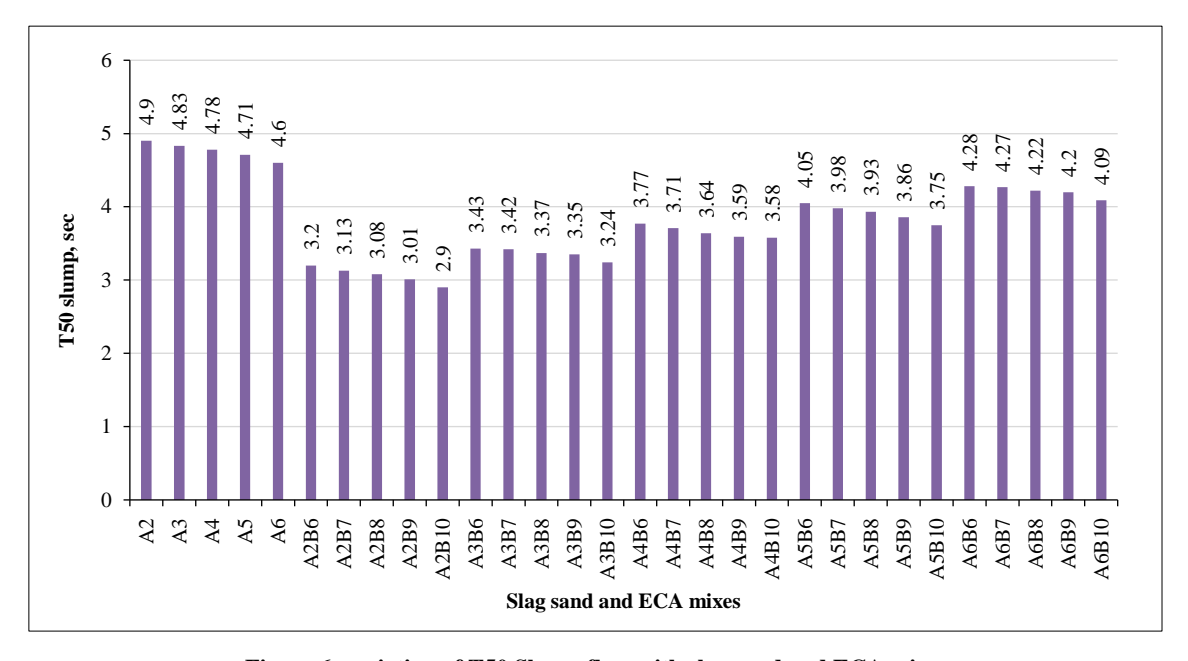


Figure 6. variation of T50 Slump flow with slag sand and ECA mixes

V-funnel flow time test: The effect of 20%, 40%, 60%, 80%, and 100% slag sand, combined with increasing proportions of expanded clay aggregate (ECA), is analyzed below and depicted in Figure 5. The V-Funnel flow time test results, illustrated in Figure 7, assess the viscosity and flow characteristics of Self-Compacting Concrete (SCC), with EFNARC guidelines recommending a flow time of less than 10 seconds for optimal performance. The control mixes (A2 to A6), which use conventional coarse aggregates and no Expanded Clay Aggregate (ECA), exhibit higher flow times ranging from 10.65 to 10.96 seconds, indicating relatively high internal friction and lower deformability. However, as ECA is introduced and its proportion increases from 20% to 100% in mixes A2B6 to A6B10, there is a marked improvement in flow behavior. The most significant enhancement is seen in mix A2B10, which records the lowest flow time of 8.59 seconds, making it the optimum mix in terms of flowability and viscosity. This performance is closely followed by A2B9 (8.97 s) and A3B10 (9.24 s), all of which fall well within the EFNARC-recommended range. The improved results are primarily due to ECA's lightweight, rounded, and porous structure, which reduces inter-particle friction and facilitates smoother flow. Although later series such as A6B10 (9.95 s) also meet the EFNARC criteria, the improvements plateau, suggesting diminishing returns at higher ECA levels. Thus, mix A2B10 emerges as the optimal blend, combining enhanced flowability and reduced viscosity while fully complying with EFNARC standards.

L-Box test: The effect of 20%, 40%, 60%, 80%, and 100% slag sand, combined with increasing proportions of expanded clay aggregate (ECA), is analyzed below and depicted in Figure 8. The graph illustrates the L-Box values of various Self-Compacting Concrete (SCC) mixes incorporating different proportions of Expanded Clay Aggregate (ECA), indicating the passing ability of the concrete. The reference mixes from A2 to A6 shows relatively lower L-Box values ranging between 0.807 and 0.828, reflecting limited flow through obstructions due to higher internal friction. As ECA is introduced from A2B6 onward, there is a significant improvement, with the L-Box value peaking at 0.898 in A2B10, which suggests excellent passing ability. This improvement is attributed to the spherical shape and lightweight nature of ECA, which reduces blocking and enhances the mixture's ability to flow around reinforcing elements. Other high-performing mixes include A2B9 (0.892), A2B8 (0.888), and A3B10 (0.884), showing consistently better

performance than mixes with traditional aggregates. However, after certain replacement levels, especially in higher series like A6B6 to A6B10, there is a slight decrease in values, stabilizing around 0.831 to 0.849. This suggests that beyond a certain ECA content, the benefits plateau or even slightly decline. Overall, A2B10 demonstrates the optimal L-Box value, confirming it has the best passing ability among all tested mixes.

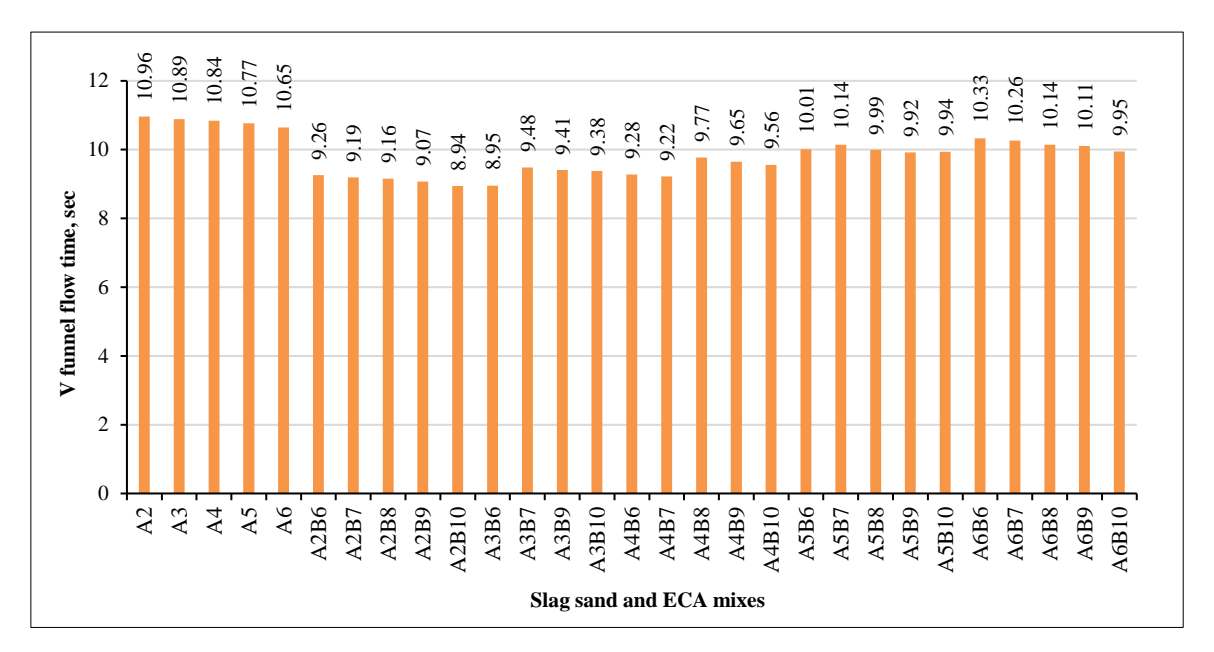


Figure 7. variation of V funnel flow time with slag sand and ECA mixes

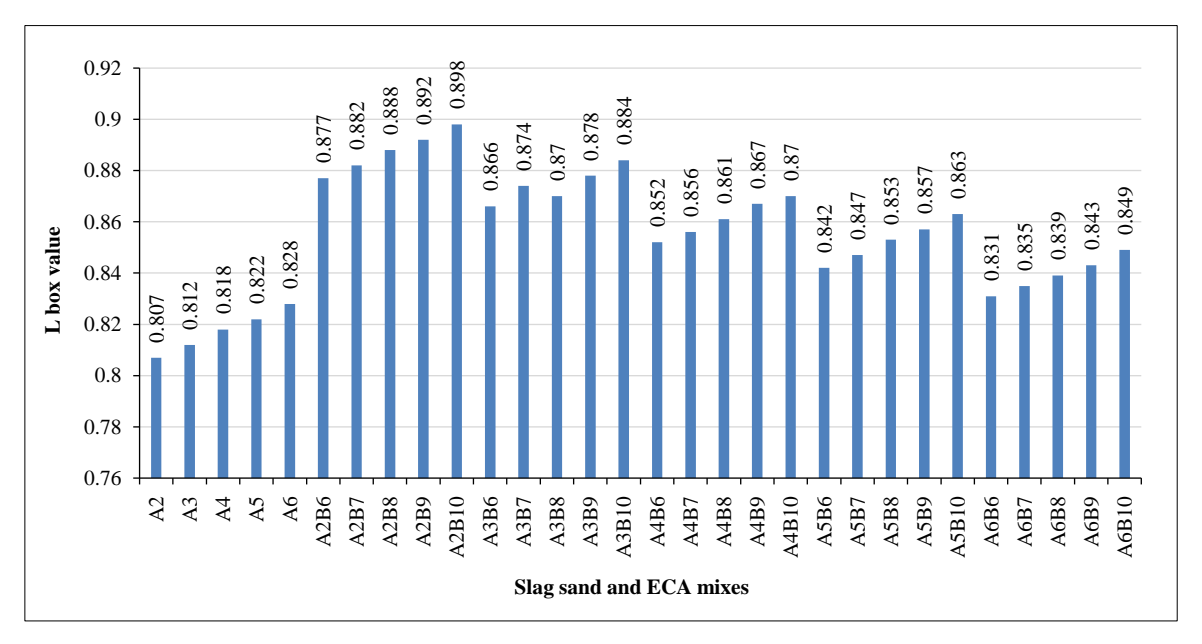


Figure 8. variation of L-box value with slag sand and ECA mixes

U-Box test: The effect of 20%, 40%, 60%, 80%, and 100% slag sand, combined with increasing proportions of expanded clay aggregate (ECA), is analyzed below and depicted in Figure 9. According to EFNARC guidelines, the U-Box test is used to assess the filling ability of self-compacting concrete (SCC) when it flows through narrow gaps and around obstacles, with lower U-Box values ideally below 30 mm, and preferably closer to 0 indicating superior flow characteristics and minimal blockage. From the graph, the reference mixes from A2 to A6 exhibit high U-Box values ranging between 17.5 mm and 18 mm, which suggests relatively restricted flow and poor filling ability. With the incorporation of Expanded Clay Aggregate (ECA) in the mixes from A2B6 to A6B10, there is a significant drop in U-Box values, especially for A2B10 (7.5 mm) and A3B10 (7.9 mm), indicating excellent flow and compliance with EFNARC's performance criteria. These values reflect improved deformability and reduced internal resistance due to ECA's lightweight, porous, and rounded nature, which enhances particle mobility. However, at very high slag sand and ECA content as seen in mixes like A6B6 and A6B7 U-Box values increase again to 15.5 mm and 15 mm, which, while still acceptable, may hint at possible segregation or reduced cohesiveness. Therefore, the optimal mix in accordance with EFNARC standards is A2B10, as it demonstrates the lowest obstruction height and highest filling efficiency.

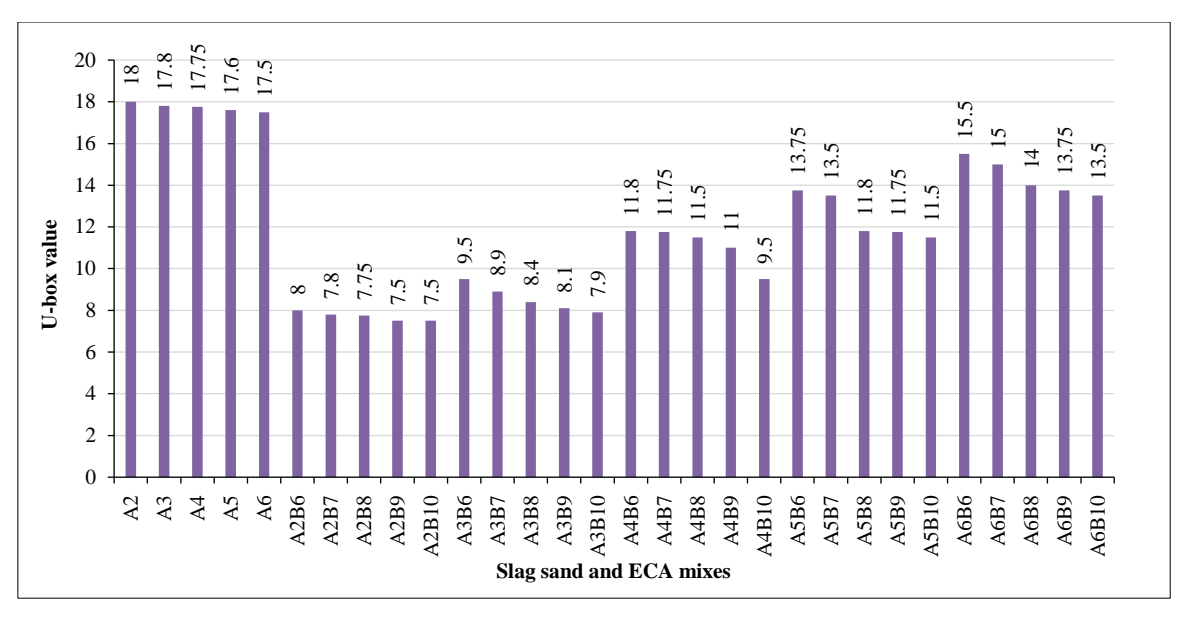


Figure 9. variation of U-box value with slag sand and ECA mixes

The improved flowability and reduced segregation observed in mixes with moderate ECA and slag sand substitution demonstrate the effectiveness of these materials in achieving SCC consistency. The enhanced cohesiveness prevented weak zones, which later influenced crack resistance in hardened specimens. Similar observations were reported [41, 42], confirming that controlled replacement levels can improve deformability while maintaining stability. This justifies the selection of ECA and slag sand as sustainable substitutes without compromising fresh performance."

3.2. Mechanical Properties

Compressive Strength: From the Figure 10., among all mixes, Mix A2B6, composed of 20% Slag Sand and 20% Expanded Clay Aggregate, demonstrated the most favorable mechanical performance. Its compressive strength reached 26.94 MPa at 7 days, increased to 42.13 MPa at 28 days, and peaked at 45.21 MPa after 90 days—outperforming all other mix variants, including the control. The results establish A2B6 as the optimum mix, achieving the highest strength across all curing durations while utilizing sustainable alternatives in both fine and coarse fractions. The moderate replacement level appears to provide a balanced internal structure, where the benefits of reduced aggregate density and improved packing are maximized without inducing excessive porosity or bond weakness. The superior performance of A2B6 can be attributed to multiple synergistic mechanisms. The partial use of slag sand, with its angularity and high fine content, may contribute to improved paste-aggregate adhesion, while the inclusion of 20% ECA introduces controlled internal curing due to its water-absorptive nature, prolonging hydration. Additionally, the pozzolanic activity from fly ash and silica fumes significantly contributes to secondary gel formation, densifying the matrix and enhancing long-term strength.

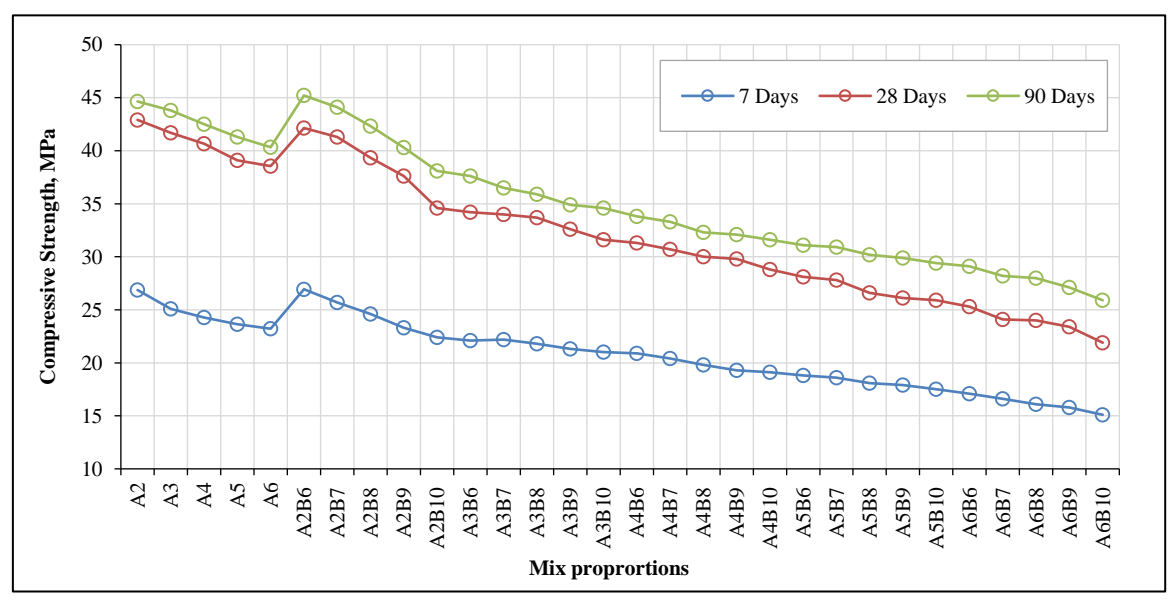


Figure 10. variation of compressive strength with slag sand and ECA mixes for different curing ages

This optimized interaction results in reduced voids and improved strength gain over time, as clearly indicated by the high 90-day strength. On the other hand, mixes with higher replacement levels, particularly those exceeding 60% ECA or 80–100% SS, exhibited a consistent decline in compressive strength. For instance, Mix A6B10 (100% SS and 100% ECA) recorded only 15.1 MPa at 7 days and 21.1 MPa at 28 days, falling below the characteristic strength limit for M30 concrete. This deterioration is likely due to the high porosity, weak interfacial transition zones, and inadequate compaction resulting from overly lightweight and absorbent aggregates, despite the presence of a high-performance binder. The observed trends are consistent with previous studies, which emphasized the importance of balancing lightweight aggregate content with binder richness and paste flow characteristics [43, 44]. The study clearly establishes that while high-volume replacements reduce the environmental footprint, they must be carefully limited to preserve structural performance. In conclusion, Mix A2B6, with 20% SS and 20% ECA, offers an optimum balance between compressive strength and material sustainability.

Split Tensile Strength: Split tensile strength tests were conducted at 7, 28, and 90 days on SCC mixes containing various levels of Slag Sand (SS) and Expanded Clay Aggregate (ECA), illustrated in Figure 11. These results supplement the compressive strength findings, offering insights into the material's tensile behavior and cracking resistance. The observed strengths ranged from 2.95 N/mm² to 5.11 N/mm², showing consistent improvement with curing age across all mixes, influenced by the ternary binder system (65% OPC, 25% Fly Ash, 10% Silica Fume) and the use of highrange water-reducing admixtures. Among the tested combinations, Mix A2B6 (20% SS + 20% ECA) once again outperformed others, recording the highest split tensile strength at all ages: 3.94 MPa (7 days), 4.93 MPa (28 days), and 5.11 MPa (90 days). This demonstrates excellent cohesion and internal tensile resistance, making A2B6 the optimum mix not only for compressive behavior but also for resistance to tensile-induced cracking. The improvement is attributed to a dense matrix formed by well-graded fines, controlled use of lightweight aggregates, and the pozzolanic reactivity of fly ash and silica fume, which refine pore structure and enhance paste-aggregate bonding. Mixes with higher aggregate replacement levels, particularly beyond 60% ECA, consistently showed reduced tensile strength. For instance, Mix A6B10 (100% SS and 100% ECA) had the lowest values, with only 2.95 MPa at 7 days and 3.87 MPa at 90 days, reflecting weak interfacial zones and internal discontinuities introduced by excessive lightweight aggregate content. The results reinforce that while ECA contributes to reduced density and enhanced sustainability, its overuse negatively affects load transfer mechanisms and cracking resistance. In summary, A2B6 is validated as the most mechanically balanced mix, exhibiting peak performance in both compressive and tensile parameters. Its dual superiority indicates optimal packing, strength development, and durability potential, positioning it as the most promising sustainable SCC mix in this study. These findings are consistent with literature indicating that moderate replacement levels of alternative aggregates can enhance tensile behavior without compromising overall matrix integrity [45, 46].

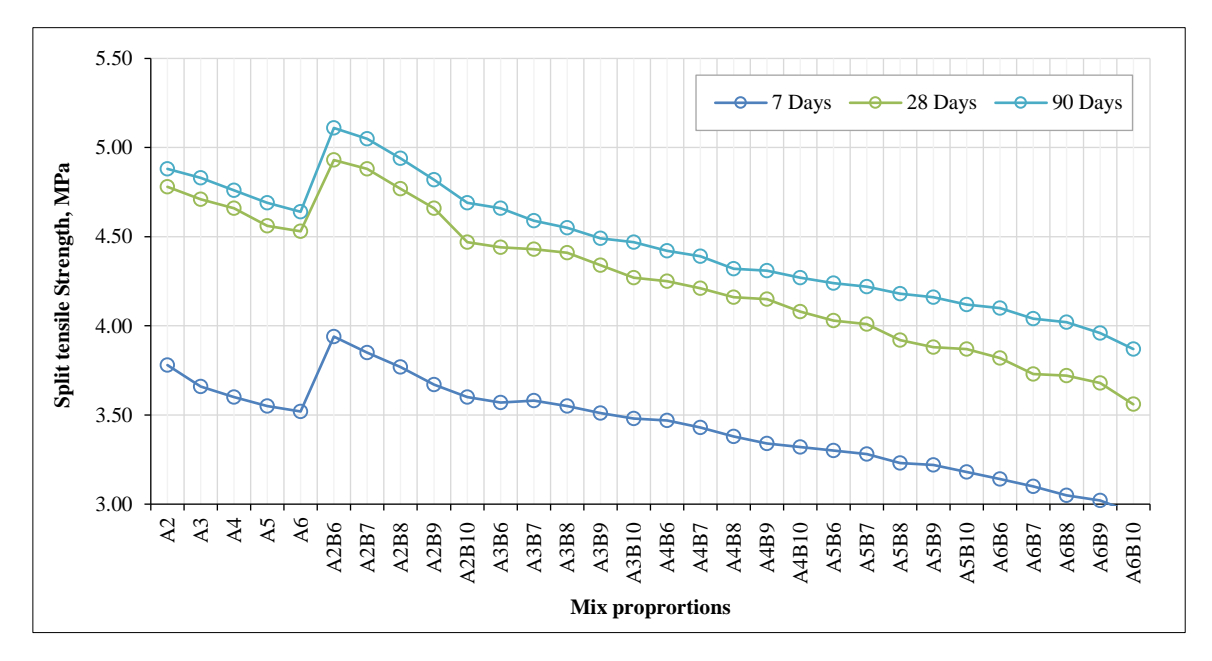


Figure 11. variation of split tensile strength with slag sand and ECA mixes for different curing ages

Flexural Strength: Flexural strength testing was performed on Self-Compacting Concrete (SCC) mixes incorporating various proportions of Slag Sand (SS) and Expanded Clay Aggregate (ECA) illustrated in Figure 12. with values ranging from 3.34 N/mm² to 5.78 N/mm² across 7, 28, and 90 days. These tests measure the concrete's ability to withstand bending stresses and resist crack growth under typical service conditions, which is particularly important for structural components such as slabs and beams. The A2B6 mix showed superior flexural strength, progressing from 4.46 MPa at 7 days to 5.55 MPa at 28 days, and achieving 5.78 MPa at 90 days. This confirms A2B6 not only as the optimum

mix in compressive and tensile domains but also as the most resistant to flexural failure. The balanced replacement 20% SS and 20% ECA likely results in optimal load dispersion along the matrix, reduced internal voids, and improved interfacial bonding due to the synergistic effect of reactive binder phases and well-graded aggregate structure. In contrast, mixes with higher replacement levels, especially those with 100% ECA (A6B10), demonstrated notably lower flexural strengths (3.34 MPa at 7 days and 4.38 MPa at 90 days). These results reflect the detrimental effect of excessive lightweight aggregate use, which leads to reduced stiffness, microcrack formation under loading, and weak aggregate-paste interaction. Additionally, Mix A3B6 (40% SS + 20% ECA) and A3B10 (40% SS + 100% ECA) showed moderate strength retention, reinforcing the benefit of keeping ECA content within 20–40% for structural applications. The performance pattern mirrors observations in compressive and tensile strength trends, confirming that optimal mechanical performance across all modes is achieved when SS and ECA are limited to moderate levels, especially when paired with a well-optimized binder system [47].

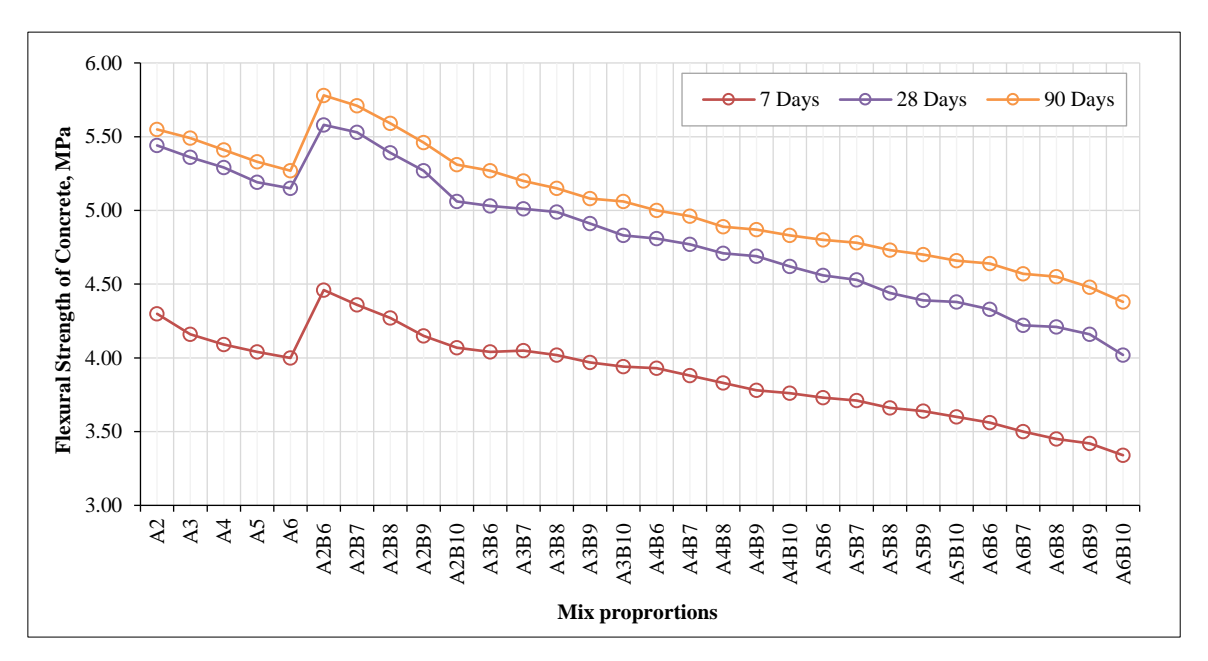


Figure 12. variation of Flexural strength with slag sand and ECA mixes for different curing ages

In compression tests, control mixes generally failed through typical cone-shaped fractures and surface spalling, whereas mixes containing slag sand exhibited narrower cracks and more gradual propagation, indicative of improved particle packing and a denser matrix. Cylindrical specimens under split tensile loading displayed longitudinal cracks along the loading axis; the crack widths were smaller in optimum mixes such as A2B6, reflecting enhanced bond strength, while higher replacement levels led to wider, more brittle cracks. Beam specimens subjected to flexural loading developed flexural cracks at the mid-span, which gradually propagated into diagonal shear cracks; mixes with ECA showed a greater number of fine cracks due to the porous aggregate structure, though the internal curing effect helped prevent sudden catastrophic failure. The strength behavior is consistent with the observed crack and failure modes. Optimum mixes (A2B6) exhibited narrower, evenly distributed cracks and gradual load transfer, reflecting denser packing and improved ITZ bonding. Higher replacement levels, however, led to wider cracks and brittle failure due to porosity. These results align with earlier findings by Revilla-Cuesta et al. [42, 45] who noted that moderate levels of recycled or lightweight aggregates enhanced strength and crack resistance. Thus, the optimum slag sand-ECA combination offers a justified balance between sustainability and performance. In addition to cubes and cylinders, prism specimens were cast and tested under flexural loading to evaluate the bending strength of the optimum SCC mix (A2B6). The prism tests provide valuable insights into the flexural behavior of the concrete, serving as an intermediate step toward structural element validation

3.3. Durability Properties

Acid Attack Test: Durability performance of SCC mixes was assessed through immersion in 5% H₂ SO₄ solution to simulate acidic exposure, with residual compressive strength measured at 28 and 90 days shown in Figure 13. The results demonstrate a general trend of strength degradation under acidic conditions, with compressive strength losses ranging from 31.02 MPa to 16.55 MPa at 28 days. The extent of deterioration is influenced by aggregate type and replacement levels. Notably, Mix A2B6 (20% SS + 20% ECA) exhibited superior acid resistance, retaining 29.91 MPa at 28 days and 27.58 MPa at 90 days, closely following the durability profile of the control mix (A2). This performance is attributed to the dense microstructure induced by the optimized binder system, which minimizes permeability and limits acid ingress. Moreover, moderate use of ECA appears to assist in mitigating internal microcrack propagation due

to its internal curing potential. Conversely, mixes with higher replacement levels (A6B10 with 100% SS + 100% ECA) suffered significant degradation, maintaining only 16.55 MPa at 28 days and dropping further to 15.30 MPa at 90 days. Such mixes likely experienced acid-induced matrix decalcification and surface leaching, exacerbated by increased porosity and reduced paste cohesion due to excessive lightweight aggregate content. Additionally, FLA-rich mixes showed lower retention compared to their counterparts, suggesting less effective acid resistance. Overall, Mix A2B6 once again confirms its optimum status, demonstrating a favorable balance between mechanical strength and durability under aggressive chemical conditions. These results align with previous studies highlighting the role of pozzolanic binders and controlled aggregate grading in enhancing acid resistance in SCC [44].

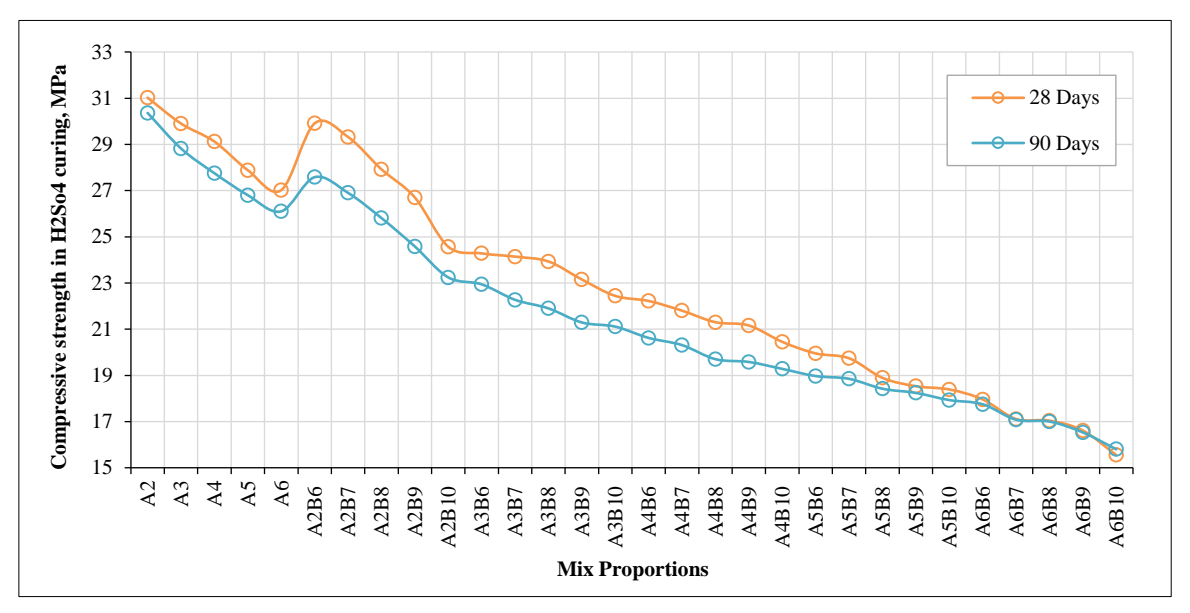


Figure 13. variation of compressive strength loss in H₂SO₄ with slag sand and ECA mixes for different curing ages

Sulphate attack Test (MgSo4): To evaluate the sulphate resistance of SCC incorporating Slag Sand (SS) and Expanded Clay Aggregate (ECA), specimens were immersed in a 5% MgSO₄ solution, and compressive strength was measured at 28 and 90 days illustrated in Figure 14. The results revealed a clear degradation pattern in all mixes under sulphate exposure, with 28-day retained strengths ranging from 35.31 MPa (A2) to 18.4 MPa (A6B10). Notably, Mix A2B6 (20% SS + 20% ECA) demonstrated the highest durability among modified mixes, retaining 35.39 MPa at 28 days and 33.91 MPa at 90 days, nearly equivalent to the control mix (A2: 35.31 MPa and 34.82 MPa, respectively). This indicates that moderate incorporation of SS and ECA does not compromise resistance to sulphate-induced deterioration. The enhanced performance of A2B6 can be attributed to its dense microstructure, reduced permeability, and strong matrix-aggregate bonding supported by the reactive pozzolanic binder system. The presence of silica fume and fly ash likely contributes to refining pore structure and reducing calcium hydroxide availability thereby limiting gypsum and ettringite formation, which are responsible for expansion and cracking under sulphate exposure.

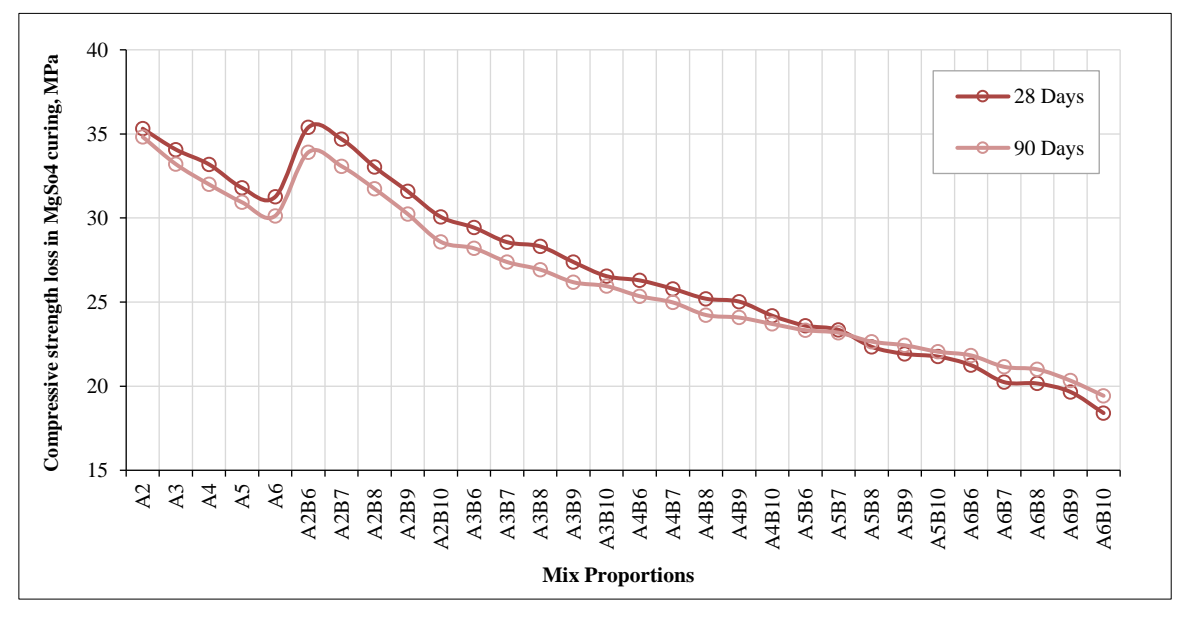


Figure 14. variation of compressive strength loss in MgSO₄ with slag sand and ECA mixes for different curing ages

In contrast, mixes with higher replacement levels (A6B10, with 100% SS and 100% ECA) exhibited significant deterioration, achieving a compressive strength of 18.4 MPa after 28 days and 19.43 MPa at 90 days. The reduced strength values suggest indicative of microstructural breakdown, high permeability, and poor durability, confirming that excessive substitution with lightweight or reactive aggregates undermines sulphate resistance. Concrete mixes containing high volumes of fly ash and lightweight aggregates suffered reduced sulphate durability due to increased porosity and soft aggregate-matrix interfaces [48]. In conclusion, Mix A2B6 demonstrates excellent sulphate resistance, closely matching control performance while enhancing sustainability. These findings reinforce the importance of moderate substitution levels and pozzolanic binder optimization to achieve long-term durability in sulphate-rich environments.

In durability tests, specimens exposed to acid and sulphate attack exhibited surface scaling and edge deterioration, with slag sand blends maintaining better integrity than controls. These observations are in line with previous findings on sustainable SCC with alternative aggregates, were optimum replacement levels improved crack control and failure resistance. Thus, the combined evidence from crack patterns, failure modes, and measured properties strongly supports the conclusion that moderate levels of slag sand and ECA enhance both mechanical performance and long-term durability. Specimens exposed to aggressive environments confirmed the durability trends, with control and optimum mixes maintaining surface integrity while higher replacements suffered scaling and deeper cracks. The improved resistance of slag sand blends is attributed to denser microstructure and reduced permeability, while ECA's internal curing mitigated sudden deterioration. Similar durability gains with controlled waste aggregate use were highlighted [49] These results justify the use of slag sand and ECA in SCC as they enhance long-term serviceability while reducing reliance on natural resources.

4. Microstructural Properties

FTIR Results and Discussion: The FTIR spectra shown in Figure 15 showed a strong band at ~970–990 cm⁻¹, characteristic of Si–O stretching vibrations in C–S–H gel. The intensity of this peak was highest for A2B6, indicating greater gel formation due to enhanced pozzolanic activity from fly ash, silica fume, and slag sand. A distinct OH stretching band near 3640 cm⁻¹, attributed to portlandite, was less intense in A2B6 compared to the control (A2), reflecting higher CH consumption during pozzolanic reactions. Carbonate peaks around 1420–1450 cm⁻¹ were present in all mixes, but slightly more pronounced in high-replacement mix A2B10, indicating greater carbonation due to higher porosity [50]. The reduction of the CH peak and enhancement of C–S–H peak in A2B6 confirm a denser and more chemically stable matrix.

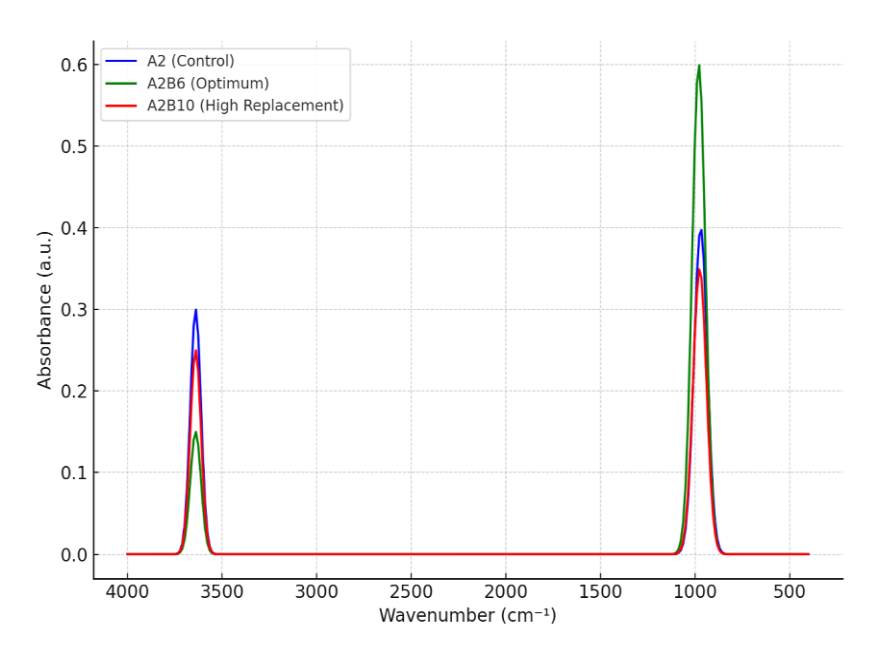


Figure 15. FTIR spectra showing C-S-H peak intensity and portlandite reduction, with A2B6 exhibiting the strongest gel formation

• TGA/DTG Results and Discussion: TGA curves illustrated in Figure 16 displayed three major weight loss regions corresponding to the identified hydration products.

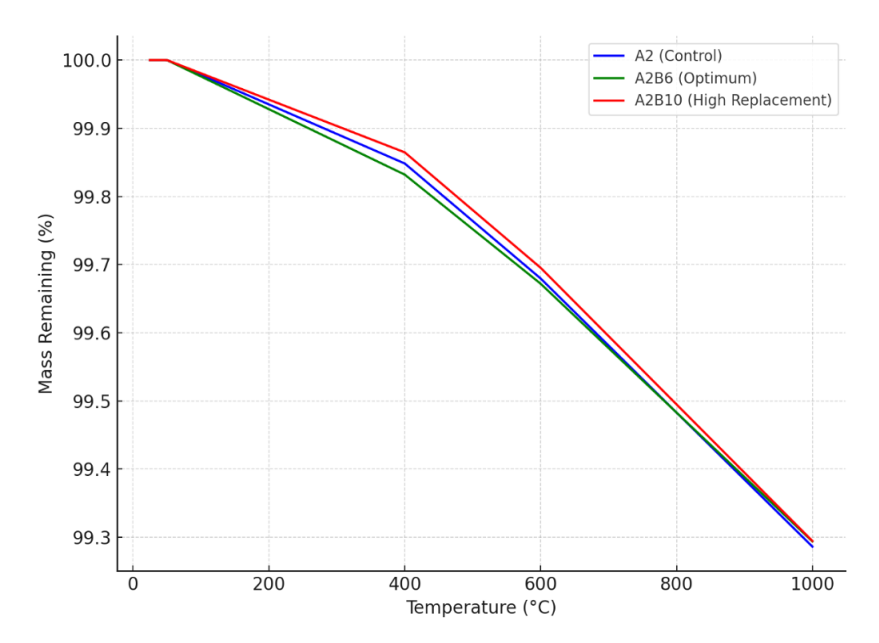


Figure 16. TGA curves illustrating higher bound water and reduced CH decomposition in A2B6, confirming its denser microstructure

- 50–200°C: A2B6 exhibited ~7.2% weight loss, higher than A2 (~6.5%) and A2B10 (~5.8%), indicating greater bound water content and thus more hydration gel.
- 400–500°C: The portlandite decomposition weight loss was lowest for A2B6 (~3.2%) compared to A2 (~4.1%), showing reduced CH presence due to pozzolanic consumption.
- 600–800°C: Carbonate decomposition losses were similar (~2.8–3.1%), with no significant impact from aggregate replacement levels.

These results align with the mechanical and durability performance, confirming that A2B6 possesses a refined pore structure and higher gel content, which enhances strength and chemical resistance.

The optimum performance of the SCC in this study was achieved with the mix A2B6, containing 20% slag sand and 20% expanded clay aggregate. This combination provided a balanced interaction between particle packing, binder reactivity, and internal curing. The partial replacement of natural sand with slag sand introduced fine angular particles that effectively filled micro voids between cement grains and natural sand, creating a denser matrix while maintaining adequate paste coating on aggregate surfaces. The 20% incorporation level proved ideal, as higher slag sand contents (>40%) increased water demand and reduced flowability, while lower contents (<20%) did not optimize void filling [51, 52]. The inclusion of expanded clay aggregate, with its porous structure, enabled internal curing by slowly releasing stored water during hydration, sustaining pozzolanic reactions over an extended period.

Its rounded particle shape also lowered interparticle friction, enhancing workability without increasing the water-to-binder ratio. The ternary binder system (65% OPC, 25% fly ash, and 10% silica fume) contributed to early-age strength from OPC, long-term strength from fly ash, and pore refinement from silica fume. The synergy between these materials in A2B6 resulted in a refined pore structure, higher C–S–H gel content, and reduced portlandite levels, as confirmed by FTIR and TGA analyses. This translated into superior mechanical properties—compressive strength of 45.21 MPa, split tensile strength of 5.11 MPa, and flexural strength of 5.78 MPa at 90 days—along with high durability, retaining 27.58 MPa after acid exposure and 33.91 MPa after sulphate exposure at 90 days. These results affirm that A2B6 not only meets structural performance requirements but also advances sustainability by reducing dependence on natural aggregates while enhancing the service life of SCC in aggressive environments. These graphical results strengthen the findings from mechanical and durability studies, clearly illustrating how slag sand and ECA contribute to matrix densification and secondary gel formation. Similar FTIR and TGA trends were reported by Islam et al. (2024) [50] and Nuruzzaman et al. (2024) [52], confirming the reliability of the present study

Microstructural studies confirmed the macroscale behaviour, as optimum mixes exhibited higher C–S–H gel formation, refined pores, and reduced portlandite, which correlate with narrower cracks and improved durability. Excessive ECA, however, showed porous zones, explaining the wider cracks and lower strength observed. These findings are in agreement with Islam et al. [50] and Renukuntla & Murthi [51] who reported that moderate inclusion of industrial by-products enhances microstructural densification. The synergy of slag sand and ECA is therefore validated, as it balances sustainability with durability and strength improvements

5. Conclusions

The following conclusions have been derived from the results and discussions:

• The experimental results clearly demonstrate that incorporating Expanded Clay Aggregate (ECA) in Self-Compacting Concrete (SCC) mixes significantly improves workability and overall performance in accordance with EFNARC guidelines. Traditional reference mixes from A2 to A6, which use only conventional coarse aggregates, exhibited limited flowability, higher viscosity, and lower passing and filling abilities. However, replacing coarse aggregates with ECA, particularly at higher percentages, resulted in substantial improvements across all fresh property tests, namely slump flow, T50, V-funnel, L-box, and U-box. Among all the combinations, mix A2B10 consistently outperformed others, achieving optimal results: a high slump flow (694 mm), low T50 time (2.9 s), reduced V-funnel flow time (8.59 s), excellent passing ability (L-box value of 0.898), and minimal obstruction height in the U-box test (7.5 mm).

- These improvements are primarily due to ECA's lightweight, rounded, and porous structure, which enhances particle mobility and reduces internal friction. Furthermore, the use of ECA promotes sustainability by reducing the demand for natural coarse aggregates and supporting the use of energy-efficient, recycled materials. Thus, A2B10 can be identified as the most effective and sustainable SCC mix, fulfilling both EFNARC performance requirements and environmental considerations.
- From the mechanical and durability performance, among the 30 mixes tested, Mix A2B6, containing 20% SS and 20% ECA, consistently demonstrated superior performance. It achieved the highest compressive strength of 45.21 MPa at 90 days, accompanied by significant values in both split tensile and flexural strengths of 5.11 MPa and 5.78 MPa, respectively. It achieved the highest compressive strength of 45.21 MPa at 90 days, along with notable split tensile and flexural strengths of 5.11 MPa and 5.78 MPa, respectively.
- Durability assessments under aggressive chemical exposures further validated the resilience of Mix A2B6. After immersion in 5% sulphuric acid (H₂SO₄) and 5% magnesium sulphate (MgSO₄) solutions, the mix retained 27.58 MPa and 33.91 MPa compressive strength at 90 days, respectively, closely aligning with the control mix. These findings underscore the efficacy of moderate SS and ECA incorporation in enhancing both the mechanical properties and chemical resistance of SCC.
- Microstructural analysis via FTIR and TGA demonstrated that the optimum mix (A2B6) had the highest C–S–H content and lowest residual portlandite, indicating advanced pozzolanic reaction and a denser matrix, which directly contributed to its superior mechanical and durability performance.
- Therefore, together, slag sand maintains stability, and ECA enhances mobility, resulting in a concrete mix that flows easily through congested reinforcement while resisting segregation. Thus, A2B10 is optimal for flow-critical applications, A2B6 emerges as the most sustainable and structurally efficient SCC mix, offering a holistic balance of workability, strength, durability, and environmental performance. This synergistic effect leads to a well-balanced SCC mix that meets both workability, stability and sustainability requirements.
- While the results demonstrate the technical viability of slag sand and ECA in SCC, further research should extend
 toward economic feasibility, embodied energy, and life-cycle sustainability assessment to comprehensively
 validate the environmental benefits of these materials.

6. Declarations

6.1. Author Contributions

Conceptualization, U.R.B. and R.B.; methodology, U.R.B.; software, U.R.B.; validation, U.R.B., R.B., and J.G.J.; formal analysis, U.R.B.; investigation, U.R.B.; resources, U.R.B.; data curation, U.R.B.; writing—original draft preparation, U.R.B.; writing—review and editing, U.R.B.; visualization, U.R.B.; supervision, R.B. and J.G.J.; project administration, R.B. All authors have read and agreed to the published version of the manuscript.

6.2. Data Availability Statement

The data presented in this study are available in the article.

6.3. Funding

The authors received no financial support for the research, authorship, and/or publication of this article.

6.4. Conflicts of Interest

The authors declare no conflict of interest.

7. References

[1] Guo, Z., Zhang, J., Jiang, T., Jiang, T., Chen, C., Bo, R., & Sun, Y. (2022). Development of sustainable self-compacting concrete using recycled concrete aggregate and fly ash, slag, silica fume. European Journal of Environmental and Civil Engineering, 26(4), 1453–1474. doi:10.1080/19648189.2020.1715847.

- [2] Gawah, Q., Al-Osta, M. A., Maslehuddin, M., Abdullah, M. A., Shameem, M., & Al-Dulaijan, S. U. (2023). Development of sustainable self-compacting concrete utilising silico manganese fume. European Journal of Environmental and Civil Engineering, 27(5), 1897–1918. doi:10.1080/19648189.2022.2102083.
- [3] Burbano-Garcia, C., Hurtado, A., Silva, Y. F., Delvasto, S., & Araya-Letelier, G. (2021). Utilization of waste engine oil for expanded clay aggregate production and assessment of its influence on lightweight concrete properties. Construction and Building Materials, 273, 121677. doi:10.1016/j.conbuildmat.2020.121677.
- [4] Ozguven, A., & Gunduz, L. (2012). Examination of effective parameters for the production of expanded clay aggregate. Cement and Concrete Composites, 34(6), 781–787. doi:10.1016/j.cemconcomp.2012.02.007.
- [5] Abdel-Raouf, M., & Abou-Zeid, M. N. (2009). Properties of concrete incorporating magnetized water. Transportation research record, 2113(1), 62-71. doi:10.3141/2113-08.
- [6] Chandra, S., & Berntsson, L. (2002). Lightweight Aggregate Concrete Microstructure. Lightweight Aggregate Concrete, 131–166, William Andrew, Norwich, United States. doi:10.1016/b978-081551486-2.50009-2.
- [7] Riccadonna, D., Walsh, K., Schiro, G., Piazza, M., & Giongo, I. (2020). Testing of long-term behaviour of pre-stressed timber-to-timber composite (TTC) floors. Construction and Building Materials, 236, 117596. doi:10.1016/j.conbuildmat.2019.117596.
- [8] Nahhab, A. H., & Ketab, A. K. (2020). Influence of content and maximum size of light expanded clay aggregate on the fresh, strength, and durability properties of self-compacting lightweight concrete reinforced with micro steel fibers. Construction and Building Materials, 233, 117922. doi:10.1016/j.conbuildmat.2019.117922.
- [9] Drouna, K., Boucetta, T. A., Maherzi, W., & Ayat, A. (2025). Enhancing the properties of expanded clay aggregates through cementitious coatings based on waste glass powder and granulated slag: Impact on lightweight self-compacting concrete performance. Construction and Building Materials, 485, 141896. doi:10.1016/j.conbuildmat.2025.141896.
- [10] Singh, R. B., Aggarwal, P., & Aggarwal, Y. (2019). Utilization of super pozzolanic material in the production of self-compacting concrete. Indian Concrete Journal, 98(2), 52–60.
- [11] Zhao, H., Sun, W., Wu, X., & Gao, B. (2015). The properties of the self-compacting concrete with fly ash and ground-granulated blast furnace slag mineral admixtures. Journal of Cleaner Production, 95, 66-74. doi:10.1016/j.jclepro.2015.02.050.
- [12] Verma, M., & Dev, N. (2022). Effect of ground granulated blast furnace slag and fly ash ratio and the curing conditions on the mechanical properties of geopolymer concrete. Structural Concrete, 23(4), 2015-2029. doi:10.1002/suco.202000536.
- [13] de Matos, P. R., Oliveira, J. C., Medina, T. M., Magalhaes, D. C., Gleize, P. J., Schankoski, R. A., & Pilar, R. (2020). Use of air-cooled blast furnace slag as supplementary cementitious material for self-compacting concrete production. Construction and Building Materials, 262, 120102. doi:10.1016/j.conbuildmat.2020.120102.
- [14] Huseien, G. F., Sam, A. R. M., & Alyousef, R. (2021). Texture, morphology and strength performance of self-compacting alkaliactivated concrete: Role of fly ash as GBFS replacement. Construction and Building Materials, 270, 121368. doi:10.1016/j.conbuildmat.2020.121368.
- [15] Singh, S., Nagar, R., & Agrawal, V. (2016). A review on Properties of Sustainable Concrete using granite dust as replacement for river sand. Journal of Cleaner Production, 126, 74-87. doi:10.1016/j.jclepro.2016.03.114.
- [16] Sravanthi, M., Venkateswara Rao, S., Krishnaveni, K., Meenuga, V. K. L., & Kariveda, S. (2022). Studies on Compressive Strength Microstructural Analysis of Self-Compacting Mortar With Bacteria. Communications Scientific Letters of the University of Žilina, 24(4), D183–D200. doi:10.26552/com.C.2022.4.D183-D200.
- [17] Deeb, R., Ghanbari, A., & Karihaloo, B. L. (2012). Development of self-compacting high and ultra-high performance concretes with and without steel fibres. Cement and Concrete Composites, 34(2), 185–190. doi:10.1016/j.cemconcomp.2011.11.001.
- [18] Kostrzanowska-Siedlarz, A., & Gołaszewski, J. (2015). Rheological properties and the air content in fresh concrete for self-compacting high performance concrete. Construction and Building Materials, 94, 555-564. doi:10.1016/j.conbuildmat.2015.07.051.
- [19] Molaei Raisi, E., Vaseghi Amiri, J., & Davoodi, M. R. (2018). Mechanical performance of self-compacting concrete incorporating rice husk ash. Construction and Building Materials, 177, 148–157. doi:10.1016/j.conbuildmat.2018.05.053.
- [20] Patil, A., Jayale, V., Arunachalam, K. P., Ansari, K., Avudaiappan, S., Agrawal, D., Kuthe, A. M., Alharbi, Y. R., Amir Khan, M., & Roco-Videla, Á. (2024). Performance Analysis of Self-Compacting Concrete with Use of Artificial Aggregate and Partial Replacement of Cement by Fly Ash. Buildings, 14(1), 143. doi:10.3390/buildings14010143.

[21] Zhao, H., Sun, W., Wu, X., & Gao, B. (2022). Sustainable self-compacting concrete containing high-amount industrial by-product fly ash as supplementary cementitious materials. Environmental Science and Pollution Research, 29(3), 3616-3628. doi:10.1007/s11356-021-15883-2.

- [22] Guo, Z., Jiang, T., Zhang, J., Kong, X., Chen, C., & Lehman, D. E. (2020). Mechanical and durability properties of sustainable self-compacting concrete with recycled concrete aggregate and fly ash, slag and silica fume. Construction and Building Materials, 231, 117115. doi:10.1016/j.conbuildmat.2019.117115.
- [23] Sasanipour, H., Aslani, F., & Taherinezhad, J. (2019). Effect of silica fume on durability of self-compacting concrete made with waste recycled concrete aggregates. Construction and Building Materials, 227, 116598. doi:10.1016/j.conbuildmat.2019.07.324.
- [24] Azizi, M., & Samimi, K. (2025). Effect of silica fume on Self-compacting Earth Concrete: Compressive strength, durability and microstructural studies. Construction and Building Materials, 472, 140815. doi:10.1016/j.conbuildmat.2025.140815.
- [25] Sheeba, K. R. J., Priya, R. K., Arunachalam, K. P., Avudaiappan, S., Maureira-Carsalade, N., & Roco-Videla, Á. (2023). Characterisation of Sodium Acetate Treatment on Acacia pennata Natural Fibres. Polymers, 15(9), 1996. doi:10.3390/polym15091996.
- [26] Kavitha, S. A., Priya, R. K., Arunachalam, K. P., Avudaiappan, S., Maureira-Carsalade, N., & Roco-Videla, Á. (2023). Investigation on Properties of Raw and Alkali Treated Novel Cellulosic Root Fibres of Zea Mays for Polymeric Composites. Polymers, 15(7), 1802. doi:10.3390/polym15071802.
- [27] Avudaiappan, S., Cendoya, P., Arunachalam, K. P., Maureira-Carsalade, N., Canales, C., Amran, M., & Parra, P. F. (2023). Innovative Use of Single-Use Face Mask Fibers for the Production of a Sustainable Cement Mortar. Journal of Composites Science, 7(6), 214. doi:10.3390/jcs7060214.
- [28] Divyah, N., Prakash, R., Srividhya, S., Avudaiappan, S., Guindos, P., Carsalade, N. M., Arunachalam, K. P., Noroozinejad Farsangi, E., & Roco-Videla, Á. (2023). Experimental and Numerical Investigations of Laced Built-Up Lightweight Concrete Encased Columns Subjected to Cyclic Axial Load. Buildings, 13(6), 1444. doi:10.3390/buildings13061444.
- [29] Raja, K. C. P., Thaniarasu, I., Elkotb, M. A., Ansari, K., & Saleel, C. A. (2021). Shrinkage study and strength aspects of concrete with foundry sand and coconut shell as a partial replacement for coarse and fine aggregate. Materials, 14(23), 7420. doi:10.3390/ma14237420.
- [30] Uysal, M., & Tanyildizi, H. (2011). Predicting the core compressive strength of self-compacting concrete (SCC) mixtures with mineral additives using artificial neural network. Construction and Building Materials, 25(11), 4105–4111. doi:10.1016/j.conbuildmat.2010.11.108.
- [31] Mohammed, M. K., Al-Hadithi, A. I., & Mohammed, M. H. (2019). Production and optimization of eco-efficient self-compacting concrete SCC with limestone and PET. Construction and Building Materials, 197, 734–746. doi:10.1016/j.conbuildmat.2018.11.189.
- [32] Bentz, D. P., & Snyder, K. A. (1999). Protected paste volume in concrete: Extension to internal curing using saturated lightweight fine aggregate. Cement and Concrete Research, 29(11), 1863–1867. doi:10.1016/S0008-8846(99)00178-7.
- [33] EFNARC. (2005). Specification and Guidelines for Self-Compacting Concrete. European Federation of National Associations Representing Concrete (EFNARC), Surrey, United Kingdom.
- [34] Okamura, H., & Ouchi, M. (2003). Self-Compacting Concrete. Journal of Advanced Concrete Technology, 1(1), 5–15. doi:10.3151/jact.1.5.
- [35] IS 516-1959. (2016). Methods of Tests for Strength of Concrete. Bureau of Indian Standards (BIS), New Delhi, India.
- [36] Neville, A.M. (2011) Properties of Concrete. Pearson Education Limited, London, United Kingdom.
- [37] Mehta, P. K., & Monteiro, P. J. (2006). Concrete microstructure, properties, and materials. McGraw-Hill Education, Columbus, United States.
- [38] Bogas, J. A., Gomes, A., & Pereira, M. F. C. (2012). Self-compacting lightweight concrete produced with expanded clay aggregate. Construction and Building Materials, 35, 1013–1022. doi:10.1016/j.conbuildmat.2012.04.111.
- [39] Zhu, W., Gibbs, J. C., & Bartos, P. J. M. (2001). Uniformity of in situ properties of self-compacting concrete in full-scale structural elements. Cement and Concrete Composites, 23(1), 57–64. doi:10.1016/S0958-9465(00)00053-6.
- [40] Siddique, R. (2008). Waste materials and by-products in concrete. Springer, Berlin, Germany. doi:10.1007/978-3-540-74294-4.
- [41] Nuruzzaman, M., Ahmad, T., Sarker, P. K., & Shaikh, F. U. A. (2023). Rheological behaviour, hydration, and microstructure of self-compacting concrete incorporating ground ferronickel slag as partial cement replacement. Journal of Building Engineering, 68, 106127. doi:10.1016/j.jobe.2023.106127.
- [42] Revilla-Cuesta, V., Manso-Morato, J., Hurtado-Alonso, N., Santamaría, A., & San-José, J. T. (2024). Degradation under cyclic wet-dry aging of full-scale high-workability concrete maximizing sustainable raw materials. Case Studies in Construction Materials, 20, e03334. doi:10.1016/j.cscm.2024.e03334.

[43] Kockal, N. U., & Ozturan, T. (2011). Durability of lightweight concretes with lightweight fly ash aggregates. Construction and Building Materials, 25(3), 1430–1438. doi:10.1016/j.conbuildmat.2010.09.022.

- [44] Rajamanickam, G., & Vaiyapuri, R. (2025). Evaluation of self compacting concrete performance incorporated with presoaked lightweight aggregates. Revista Materia, 30. doi:10.1590/1517-7076-RMAT-2024-0813.
- [45] Revilla-Cuesta, V., Skaf, M., Faleschini, F., Manso, J. M., & Ortega-López, V. (2020). Self-compacting concrete manufactured with recycled concrete aggregate: An overview. Journal of Cleaner Production, 262, 121362. doi:10.1016/j.jclepro.2020.121362.
- [46] Thomas, M.D.A. (2007) Optimizing the Use of Fly Ash in Concrete. Portland Cement Association, Skokie, United States.
- [47] Mansur, A. Z., Djamaluddin, R., Parung, H., & Irmawaty, R. (2024). Study of Post-Spalling Reinforced Concrete Beam Repair Using Grouting and GFRP Reinforcement. Civil Engineering Journal, 10(1), 131–144. doi:10.28991/CEJ-2024-010-01-08.
- [48] Jena, S., & Panigrahi, R. (2022). Evaluation of Durability and Microstructural Properties of Geopolymer Concrete with Ferrochrome Slag as Coarse Aggregate. Iranian Journal of Science and Technology Transactions of Civil Engineering, 46(2), 1201–1210. doi:10.1007/s40996-021-00691-y.
- [49] Qin, D., Zong, Z., Dong, C., Guo, Z., Tang, L., Chen, C., & Zhang, L. (2023). Long-term behavior of sustainable self-compacting concrete with high volume of recycled concrete aggregates and industrial by-products. Structural Concrete, 24(3), 3385-3404.
- [50] Islam, S., Ara, G., Akhtar, U. S., Mostafa, M. G., Haque, I., Shuva, Z. M., & Samad, A. (2024). Development of lightweight structural concrete with artificial aggregate manufactured from local clay and solid waste materials. Heliyon, 10(15), 34887. doi:10.1016/j.heliyon.2024.e34887.
- [51] Renukuntla, A., & Murthi, P. (2024). Bibliometric analysis on Characterization of Sustainable lightweight Self Compacting Concrete with Recycled Aggregate. E3S Web of Conferences, 559, 04001. doi:10.1051/e3sconf/202455904001.
- [52] Nuruzzaman, M., Almeida, J., Amin, M. T. E., & Sarker, P. K. (2024). Performance of Sustainable Green Concrete Incorporating Quarry Dust and Ferronickel Slag as Fine Aggregate. Materials, 17(10), 2326. doi:10.3390/ma17102326.